Transport properties of bismuth sulfide single crystals

A. Cantarero, J. Martinez-Pastor, and A. Segura
Departamento de Física Aplicada, Facultad de Fisica, Burjasot (Valencia), Spain

A. Chevy
Laboratoire de Physique des Milieux Très Condensés, Université de Paris VI, 4 Place Jussieu Tour 13, 75230 Paris Cedex 05, France

(Received 9 December 1986)

Impurity levels and electron scattering mechanisms in bismuth sulfide have been investigated by means of resistivity and Hall-effect measurements in the 30—500-K temperature range. Lattice scattering is predominant in this range and the temperature dependence of the electron mobility, in the crystallographic directions a and c, has been quantitatively interpreted through Fivaz-Schmid and Brooks-Herring models for homopolar optical phonon and ionized impurities scattering, respectively, yielding the energy of the phonon mode ($\hbar\omega = 14$ meV) and the electron-phonon coupling constant ($g^2 \gtrsim 0.4$). The density-of-states effective mass in the conduction band has also been determined from Seebeck-effect measurements at room temperature.

I. INTRODUCTION

Bismuth sulfide (Bi_2S_3) is a layered semiconductor that crystallizes in the orthorhombic system (*Pbnm* space group) and is isostructural to Sb_2S_3 and Sb_2Se_3.[1] Its energy gap is about 1.45 eV at room temperature, then near to the optimum for photovoltaic conversion. It has been proposed as a good electrode for liquid-junction solar cells.[2–4]

The transport properties of Bi_2S_3 single crystals are poorly known. Only a few reports on this subject have been published up to now. Gildart *et al.*[5] have performed thermopower, thermal conductivity, and resistivity measurements in the 300—400 °C range, but do not conclude anything about scattering mechanisms. Vinogradova *et al.*[6] investigated transport properties of Bi_2S_3 between 100 and 300 K and reported a temperature dependence of electron mobility in the form $\mu \propto T^{-m}$ with m varying from 0.5 to 1. The electron concentration of their samples being very high (of the order of 10^{20} cm^{-3}), their discussion and conclusions about scattering mechanisms, in terms of the theory for nondegenerate semiconductors, do not seem to be well founded. Glatz and Meikleham[7] report Hall-effect and resistivity measurements, ranging from 78 to 300 K in temperature, with current flowing along the c axis, and thermopower and thermal conductivity measurements at room temperature. No anisotropy of electron mobility is observed and its temperature dependence is found to be $\mu \propto T^{-1.64}$ but no interpretation is proposed. Heckman and Mattox[8] report resistivity and Hall-effect measurements between −60 and 80 °C. They point out that their results are irreproducible. We have not found any reference to anisotropy in transport properties of Bi_2S_3.

In this paper we report resistivity and Hall-effect measurements in oriented single crystals of Bi_2S_3 between 30 and 500 K and thermopower measurements at room temperature in Sec. III. Section IV is devoted to the interpretation of these results by means of the Fivaz-Schmid theory for homopolar optical-phonon scattering in layered semiconductors[9,10] and Brooks-Herring theory for ionized impurity scattering.[11,12]

II. EXPERIMENTAL

Bismuth sulfide single crystals used in this work have been grown by the Bridgman method from a stoichiometric polycrystalline melt, with a temperature gradient of 120 °C/cm and a growth velocity of 0.5 mm/h. The purity of the elements was 99.9% for Bi and 99.9998% for S.

Samples were prepared by cleaving from the ingot with a razor blade. It must be pointed out that mirror surfaces parallel to the a-c plane are obtained only when the cleaving strength is applied in the direction of the a axis, otherwise the surface of the sample appears as grooved in the c-axis direction. The samples obtained in this way are parallelepipedal shaped and so easily oriented, because Bi_2S_3 also cleaves in the b-c plane. Ohmic contact in the classic configuration for parallelepipedal samples were prepared by vacuum deposition of bismuth. The current density was parallel to the c axis or to the a axis. It was not possible to prepare slabs with faces parallel to the b axis due to the weakness of bonds in this direction.[13] The size of the samples was typically 3×6 mm^2. The thickness ranged between 70 and 140 μm and it was obtained from the interference fringe pattern in the infrared transmission spectrum (between 2 and 2.5 μm in wavelength).

Measurements between 30 and 300 K were carried out in a closed-cycle Leybold cryogenic system with a magnetic field strength of 0.6 T. Measurements at high temperature (300—500 K) were made only for one of the samples in a standard system, the magnetic field strength being 0.4 T. The noise level was very high and the Hall-effect measurement was not accurate. So the carrier con-

TABLE I. Comparison between electron concentration, Hall mobility, and the slope of μ_H at 30, 70, and 300 K.

		30 (K)			70 (K)			300 (K)		
Sample	Crystal direction	n (10^{16} cm^{-3})	μ_H (cm^2/V s)	m	n (10^{16} cm^{-3})	μ_H (cm^2/V s)	m	n (10^{16} cm^{-3})	μ_H (cm^2/V s)	m
Bi-1	a				2.9	110	1.6	6.35	8.6	1.8
Bi-2	a	1.23	239	0.6	2.2	107	2.03	4.46	7.9	1.55
Bi-3	a	2.68	516	1.54	5.6	120	1.63	8.47	11.0	1.82
Bi-4	c	1.61	889	0.57	3.7	370	1.71	3.85	31.2	1.63
Bi-5	c	1.44	1001	1.1	1.9	480	1.67	3.03	25.0	1.81
Bi-6	c	1.98	1058	0.76	3.75	400	1.76	6.34	28.0	1.61

centration at high temperature was calculated from the experimental resistivity and extrapolated values of mobility, calculated from the complete formula that fits them in the 30—300 K temperature range.

For Seebeck-effect measurements the sample was mounted between two aluminum blocks. The cold one remained in thermal contact with the cold head of the cryogenic system at a stabilized temperature. The hot one was thermal and electrically insulated from the cold head and was heated with a carbon resistor. The temperature difference was measured with a copper-Constantan thermocouple. The Seebeck coefficient was obtained by an improved slope method.[14]

III. RESULTS

A. Carrier concentration

Hall mobility μ_H is less than 1000 cm^2/V s in the measured temperature range and the strength of the magnetic field was 0.6 T. The product $\mu_H^2 B^2$ is always lower than 4×10^{-3} and we can neglect $\mu_H^2 B^2$ in front of 1. In that approximation, carrier concentration is

$$n = A/eR_H \ , \tag{1}$$

where R_H is the Hall constant, e the electron charge, and A the Hall ratio that we have taken to be 1, as we will discuss in Sec. IV.

Figure 1 shows the electron concentration as calculated from expression (1) versus the inverse temperature for several samples. The behavior of all the samples is similar. There is a first zone from 30 to 40—50 K in which n increases with temperature, a second zone, from 50 to 100 K in which n is nearly constant and a third part for temperature higher than 100 K in which n increases again with temperature. No linear zone in the Arrhenius plot appears in the explored temperature range for any sample.

B. Mobility

Figure 2 shows the electron Hall mobility results for six samples of Bi_2S_3. The electron Hall mobility in the a- and c-axis directions was obtained from the resistivity and Hall-coefficient results in samples where current flows parallel to a and c axes, respectively. Around a given temperature T_0, μ_H can be expressed in function of T in

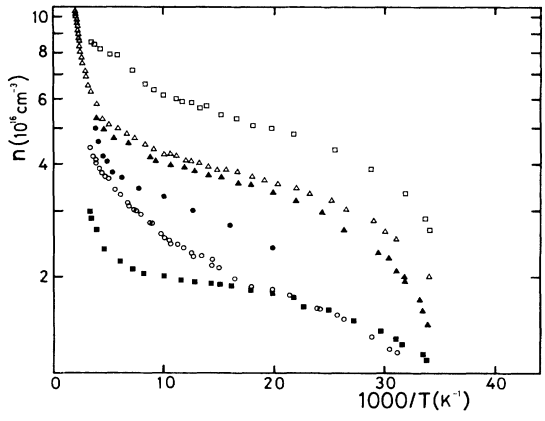

FIG. 1. Electron concentration for six samples of Bi_2S_3 as a function of temperature. ●, Bi-1; ○, Bi-2; □, Bi-3; ▲, Bi-4; ■, Bi-5; △, Bi-6.

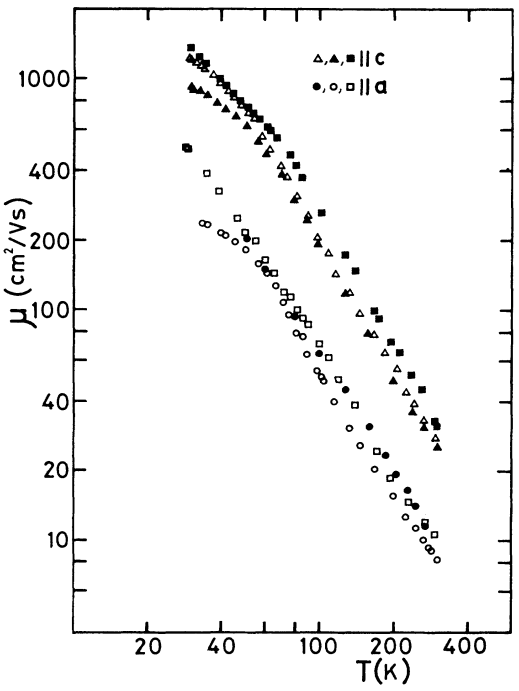

FIG. 2. Hall mobility of Bi_2S_3 vs temperature. ●, Bi-1; ○, Bi-2; □, Bi-3; ▲, Bi-4; ■, Bi-5; △, Bi-6.

TABLE II. Seebeck coefficient and electron concentration used in the least-square procedure for obtaining m_d^*.

Sample	n (10^{16} cm^{-3})	α (μV/K)
a	25	550
Bi-1	8.5	600
Bi-4	5	650
Bi-6	4	690
Bi-7	1.5	750

[a]From Ref. 5.

the following form:

$$\mu_H(T)=\mu_H(T_0)(T/T_0)^{-m}. \quad (2)$$

In that expression m represents the slope of the double logarithmic plot $\mu_H(T)$. The slope m increases from 1.7 to 2.1 as temperature decreases from 300 to 70 K. Below 70 K m decreases but does not change sign in the studied temperature range.

The electron Hall mobility turns out to be anisotropic. The higher value corresponds to the c direction and the anisotropy ratio is $\mu_{H,c}/\mu_{H,a}=3.0\pm0.5$. Table I shows the values of electron Hall mobility, carrier concentration, and the slope m at 30, 70, and 300 K. It must be pointed out that the electron Hall mobility and the slope do not necessarily increase for lower electron concentration.

C. Thermoelectric power

Table II shows the Seebeck coefficients measured at room temperature for several samples of Bi_2S_3, and the electron concentration, as obtained from Hall-effect measurements through Eq. (1) with $A=1$.

IV. DISCUSSION

A. Impurity levels

The fact that n is nearly constant between 40 and 100 K and no linear region appears in the Arrhenius plot below and above those temperatures, indicates that the impurities contained in the Bi_2S_3 crystals here studied are near to complete ionization or starting the ionization in that temperature range. The low-temperature region should then correspond to the exhaustion of a shallow level with low ionization energy (lower than 10 meV). The high-temperature region may be related to the onset of the ionization of a deep donor level with ionization energy higher than 100 meV. The last value was obtained from the slope of the Arrhenius plot for the sample Bi-6 at 500 K (see Fig. 2). The presence of compensating impurities in those samples is revealed by the fact that electron mobility is not necessarily lower for higher electron concentration at 30 K (see Table I). A model including two donor levels and an acceptor level would then be necessary to fit the experimental results. Nevertheless, given the smooth temperature dependence of n, the interval of variation of the parameters that fit the results is so large that it does not give more information than the qualitative analysis attempted in this section.

The optical-absorption edge of Bi_2S_3 at 30 K exhibit an exciton peak whose binding energy is of the order of 30 meV.[15] On the other hand, the ionization energy of an hydrogenoid impurity should be of the same order or higher than the binding energy of the exciton (depending on the ratio of electron effective mass to hole effective mass). According to our analysis in the last paragraph, the ionization energy of shallow donors in Bi_2S_3 should be lower than 10 meV. The presence of compensating acceptors may explain this anomaly through the formation of donor-acceptor pairs in which the ionization energy may be much lower than in the isolated donor.[16]

The deep donor level may be related to an impurity absorption band centered at a photon energy of 321 meV that is observed in the infrared transmission spectrum of these samples at room temperature.[17] The onset of the ionization of a deep donor with such ionization energy is compatible with the increase of the electron concentration above 200 K.

As regards the acceptor impurities, a weak impurity absorption band is observed at low temperature just below the fundamental absorption edge at a photon energy of 1.37 eV at 30 K,[15] which may correspond to a transition from an acceptor level (located 170 meV above the valence band) to the conduction band.

A word must be said about the influence of purity of the elements used in the synthesis of the compound. Using low-purity Bi does not degrade the optical and transport properties of the crystal due to the high-impurity segregation coefficient of layered materials.[18] In fact, the electron mobility in the samples here studied is higher than in other references in literature and has been found to be determined by lattice vibrations and not by ionized impurities between 30 and 300 K (Ref. 15) which confirms the quality of these crystals. This is also the case for the optical-absorption edge where intensity and width of the exciton peak that appears below 100 K is also lattice controlled.[15]

B. Electron scattering mechanisms

Layered semiconductors have in general low structural symmetry, so homopolar optical phonons can produce very strong deformation potentials and then be strongly coupled to electrons. The Fivaz-Schmid model[9,10] for homopolar optical-phonon scattering is based on this hypothesis, and has been proved to explain quite well the temperature dependence of electron and hole mobility in III-VI layered semiconductors.[10,19] In the case of Bi_2S_3 the site symmetry is much lower than in the III-VI compounds; then we have used that model to interpret the temperature dependence of electron mobility in Bi_2S_3. But given that the Fivaz-Schmid model foresees a continuous increase of the slope m with decreasing temperature, we must also take into account the ionized impurity scattering, that we incorporate through the Brooks-Herring relaxation time.[12]

The electron drift mobility in the i direction for both scattering mechanisms would be

$$\mu_{d,i}=e\langle\tau\rangle/m_i^* = (4e/3\sqrt{\pi}m_i^*\int_0^\infty \tau(u)\exp(-u)u^{3/2}du \ , \quad (3)$$

where

$$u=E/kT \ , \quad (4)$$

m_i^* is the electron effective mass in the i direction and

$$1/\tau=1/\tau_{\rm BH}+1/\tau_{\rm FS} \ , \quad (5)$$

$\tau_{\rm BH}$ and $\tau_{\rm FS}$ being the relaxation times corresponding to the models of Brooks-Herring[12] and Fivaz-Schmid,[10] respectively.

The electron Hall mobility can be expressed by

$$\mu_{H,i}=A\mu_{d,i} \quad (6)$$

and

$$A=\langle\tau^2\rangle/\langle\tau\rangle^2 \ . \quad (7)$$

We assumed the Hall factor A to be a unit in order to calculate the electron concentration. As the electron Hall mobility increases with decreasing temperature in the whole studied range the predominant mechanism must be the phonon scattering. For the Fivaz-Schmid relaxation time, $A=1$ for $kT\ll\hbar\omega_{\rm ph}$ and $A=1.18$ for $kT\gg\hbar\omega_{\rm ph}$. Taking into account the temperature dependence of A would introduce a very small change in the slope of the double logarithmic plot, which is the most significative parameter in order to study the scattering mechanisms, and m is, in this case, determined by the phonon energy. Therefore, taking $A=1$ would practically not affect this fitting parameter. The error introduced by taking $A=1$ in the phonon energy, which gives the absolute value of the electron mobility, would be lower than the dispersion of experimental results. Thus we have fitted the theoretical Eq. (3) to the experimental results for the samples with a maximum mobility in both directions. In this calculation we have used the measured values of the electron concentration in each sample. The ionized impurity concentration has been taken to be

$$N_i=n+2N_a \ , \quad (8)$$

where we have introduced N_a compensating acceptors. The ionized donors must compensate the free electrons as well as the ionized acceptors, according to the neutrality condition, which justifies the factor 2 in Eq. (8). The presence of the acceptors is also necessary in order to give quantitative account of the fact that electron mobility can be lower in samples with lower electron concentration. In the explored range of temperatures the fit is quite unsensible to relatively large variations of the parameters included in the screening term of the Brooks-Herring relaxation time. We have chosen the trial value of ϵ_0 to be the high-frequency dielectric constant and m_d^* to be the rough value of the effective mass as obtained from thermoelectric measurements without taking into account the scattering term in Eq. (9). With this assumption, four fitting parameters must be determined: $g^2m_i^*$, $\hbar\omega_{\rm ph}$, N_a, and $\epsilon^2(m_d^*)^{1/2}/m_i^*$. The first approximation can be estimated as follows. From the slope of the double logarithmic plot $h\omega_{\rm ph}$ may be obtained. With this value, the 300-K electron mobility gives an estimation of $g^2m_i^*$. The reduction of low-temperature mobility with respect to the value in absence of impurity scattering gives N_a and $\epsilon^2(m_d^*)^{1/2}/m_i^*$. With this first analysis a χ^2 procedure leads very quickly to the best-fit parameters that appear in Table III for the samples with highest electron mobility in each direction (Bi-2 and Bi-6 in Table I). In Fig. 3 we compare the experimental results with the theoretical mobility as calculated through Eq. (3) with the parameters given in Table III. The calculated mobility perfectly fits the experimental results through the whole temperature range here explored.

In order to extract some physical information about fundamental parameters of Bi_2S_3, Seebeck-effect results must be interpreted. Once we have found a scattering mechanism model to give account of $\mu_H(T)$ results, it is possible to obtain the conduction-band density of states effective mass from thermopower measurements. The Seebeck coefficient for a nondegenerate n-type semiconductor is given by[20]

$$\alpha=(k/e)[\langle\tau E\rangle/kT\langle\tau\rangle+\ln N_c/n] \ . \quad (9)$$

We have calculated $\langle\tau E\rangle/kT\langle\tau\rangle$ at room temperature and for n and N_i in the range of values found here. It turns out to be constant. Given that n is known in each sample from Hall-effect measurements we can calculate N_c and determine the density of states electron effective mass that is $m_d^*=(0.68\pm0.05)m_0$. With this value and

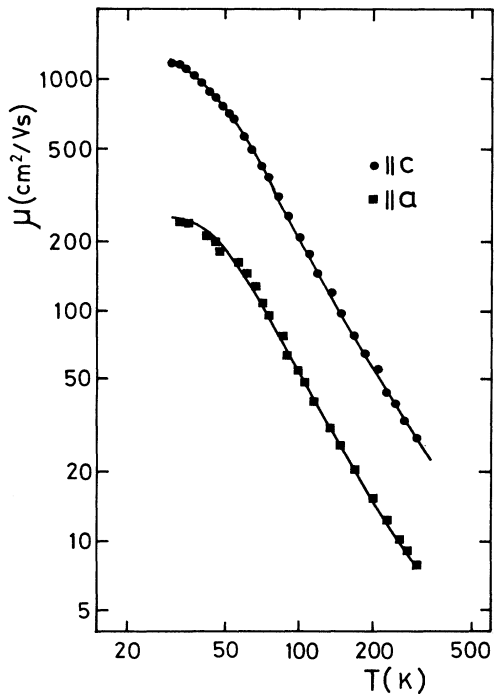

FIG. 3. Theoretical fitting of $\mu_H(T)$ curves from expression (3).

TABLE III. Parameters obtained from the fitting of mobility curves using the *F-S* and *B-H* models.

Sample	Crystal direction	$g^2 m_i^*$	$\hbar\omega_{ph}$ (meV)	N_a (10^{15} cm^{-3})	$\epsilon^2 (m_d^*)^{1/2}/m_i^*$
Bi-2	*a*	0.876	14.0	8.5	96.4
Bi-6	*c*	0.240	14.0	5.0	352

the results of mobility fit, several consequences can be extracted.

(i) The $\mu_H(T)$ curves for *a* and *c* directions are nearly identical, especially between 300 and 100 K besides the absolute value. It seems reasonable to attribute the mobility anisotropy to electron effective-mass anisotropy, being the anisotropic ratio $m_a^*/m_c^* = \mu_{H,c}/\mu_{H,a} = 3.0 \pm 0.5$. This result is consistent with the fact that chemical bonds in Bi_2S_3 crystals are very anisotropic. Covalent bonds are directed along the *c* axis. Along the *a* and *b* directions binding is made by weaker ionic and Van der Waals forces.

(ii) From optical measurements a mean value of the high-frequency dielectric constant of Bi_2S_3 has been obtained,[17] $\epsilon_\infty = 10.9$. Given that the static dielectric constant must be higher than ϵ_∞, we can give an upper limit for both effective masses from the fit parameter $\epsilon^2 (m_d^*)^{1/2}/m_i^*$ given in Table II. We obtain $m_c^* < 0.6 m_0$ and $m_a^* < 2.2 m_0$.

(iii) With these results and the fitting parameter $g^2 m_i^*$ given in Table II (column 2), we can give a minimum value for the electron-phonon coupling constant $g^2 > 0.4$.

(iv) The low electron mobility in this material appears then to be an intrinsic property due to the high electron effective mass and strong electron-phonon coupling.

V. CONCLUSIONS

Transport properties of bismuth sulfide single crystals have been investigated. The smooth temperature dependence of electron concentration has allowed only an estimation of the ionization energy of donor levels. One shallow level at less than 10 meV below the conduction band and one deep level with ionization energy higher than 100 meV has been identified in these samples. On the opposite, the strong temperature dependence of electron mobility could be quantitatively interpreted through the Fivaz-Schmid model for homopolar phonon scattering (which is the predominant mechanism) and the Brooks-Herring model for ionized impurity scattering which must also be taken into account. The anisotropy can be attributed to the electron effective-mass anisotropy ($m_a^*/m_c^* = 3$). The energy of the homopolar phonon mode coupled to electrons has been determined as well as the electron-phonon coupling constant. Density of states electron effective mass has also been determined from Seebeck-effect measurements. The main conclusion of this work is that the low electron mobility is not due to the presence of defects in the material but seems to be an intrinsic property of this semiconductor.

[1] W. Hofmann, Z. Kristallogr., **86**, 225 (1933).

[2] D. D. Miller and A. Heller, Nature **262**, 280 (1976).

[3] P. A. Krishna and G. K. Shivakumar, Thin Solid Films **121**, 151 (1984).

[4] P. A. Krishna, J. Mater. Sci. Lett. **3**, 837 (1984).

[5] L. Guildart, J. M. Kline, and D. M. Mattox, J. Phys. Chem. Solids **18**, 286 (1961).

[6] M. N. Vinogradova, O. A. Golikova, B. A. Efimova, V. A. Kutasova, T. S. Stavitskaya, L. S. Stil'bans, and L. M. Sysoeva, Fiz. Tverd. Tela **1**, 1333 (1959).

[7] A. C. Glatz and V. F. Meikleham, J. Electrochem. Soc. **110**, 1231 (1963).

[8] R. C. Heckmann and D. M. Mattox, J. Phys. Chem. Solids **24**, 973 (1963).

[9] Ph. Schmid, Il Nuovo Cimento, **21**, 258 (1974).

[10] R. C. Fivaz and Ph. E. Schmid, *Optical and Electrical Properties* (Reidel, Dordrecht, 1976), Vol. 4.

[11] H. Brooks, Phys. Rev. **83**, 879 (1951).

[12] A. Chattopadhyay and H. J. Queisser, Rev. Mod. Phys. **53**, 745 (1981).

[13] E. Mooser and W. B. Pearson, J. Phys. Chem. Solids **7**, 65 (1958).

[14] A. Casanovas, A. Cantarero, A. Segura, and A. Chevy, Phys. Status Solidi A **92**, K155 (1985).

[15] A. Cantarero, Doctoral thesis, University of Valencia, Spain, 1986.

[16] A. C. Beer, *Semiconductors and Semimetals* (Academic, New York, 1975), Vol. 10.

[17] A. Cantarero, A. Segura, J. Martínez-Pastor, and A. Chevy, Phys. Status Solidi A (to be published).

[18] A. Chevy, These d'Etat, University of Paris VI, 1981.

[19] A. Segura, F. Pomer, A. Cantarero, W. Krause, and A. Chevy, Phys. Rev. B **29**, 5708 (1984).

[20] K. Seeger, *Semiconductor Physics*, Vol. 40 of *Springer Series in Solid State Sciences* (Springer-Verlag, Berlin, 1982).